Spatial distribution of the wave functions of a graphite surface studied by use of metastable-atom electron spectroscopy

S. Masuda, H. Hayashi, and Y. Harada
Department of Chemistry, College of Arts and Sciences, The University of Tokyo, 3-8-1 Komaba, Meguro-ku, Tokyo 153, Japan
(Received 6 March 1990; revised manuscript received 9 April 1990)

Rare-gas metastable atoms (He*,Ne*,Ar*) were shown to deexcite on a graphite surface via the direct Auger deexcitation process. This is the first observed case in which the resonance ionization of the metastable atoms is suppressed on the surface with empty levels having the same energy as those of the highest occupied levels of the metastable atoms. The electron emission spectra correlate closely with the density-of-states maxima originating from the π bands, while the contribution from the sp^2-hybridized σ bands is almost missing. These findings can be interpreted in terms of the spatial distribution of the wave functions of the graphite surface.

I. INTRODUCTION

The nature of wave functions localized on solid surfaces plays an important role in the surface properties and has, therefore, received considerable attention for many years. Although the band dispersion (binding energy versus wave vector) and the symmetry of the wave function have been well studied by use of photoemission and inverse-photoemission measurements, etc., information on the spatial distribution of the wave function is rather limited. In this paper we wish to demonstrate that such information can be obtained by means of metastable-atom electron spectroscopy, in which the kinetic energy of electrons emitted by thermal collisions of rare-gas metastable atoms with solid surfaces is analyzed. For this purpose we have taken up graphite as a sample, because it is a typical two-dimensional solid and the band structure is rather simple.

According to Hagstrum,[1] rare-gas atoms are deexcited on the solid surfaces via one of the following two mechanisms shown in Fig. 1. (a) On a metal or semiconductor surface, in which empty levels lie opposite the excited level of the metastable atom, the electron in the excited level resonantly tunnels into an empty level of the surface [resonance ionization (RI); see Fig. 1(a_1)]. The remaining positive ion is then neutralized by an Auger transition [Auger neutralization (AN); see Fig. 1(a_2)]. (b) On an insulator or adsorbate-covered metal surface having no empty level opposite the excited level of the metastable atom, the RI process is suppressed and the metastable atom is deexcited by an Auger deexcitation (AD) or Penning ionization (PI) process, in which an electron from an occupied level of the surface fills the hole of the metastable atom and its excited electron is emitted simultaneously.

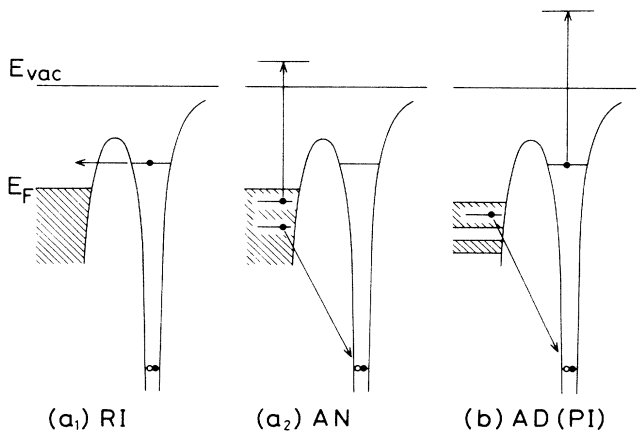

FIG. 1. Deexcitation mechanisms of a metastable atom. (a_1) and (a_2) show resonance ionization (RI) followed by Auger neutralization (AN) on a metal or semiconductor surface. (b) shows Auger deexcitation (AD) or Penning ionization (PI) on an insulator surface.

In the present study we found that the metastable atoms (He*, Ne*, and Ar*) relax into the ground states on the graphite surface through direct AD process. This is the first case in which the surface with empty levels having the same energy as those of the highest occupied levels of the metastables is found to show deexcitation via the AD process. Further, the electron-emission spectra correlate closely with the density of states originated from π (C $2p_z$) bands, while the contribution from the sp^2-hybridized σ bands is almost missing. These findings can be interpreted on the basis of the spatial distribution of the occupied and unoccupied wave functions of graphite, i.e., the wavelength and amplitude of Bloch functions.

II. EXPERIMENT

The details of the experimental apparatus and related procedure have been described elsewhere.[2,3] The metastable-atom electron spectra (MAES) and ultraviolet-photoemission spectra (UPS) were measured by a 180° hemispherical-type analyzer with an acceptance angle of ±2°. Overall energy resolution was about 0.2 eV. Metastable atoms (He* $2\,^1S$, 20.62 eV and $2\,^3S$, 19.82 eV; Ne* $^3P_0$, 16.72 eV and $^3P_2$, 16.62 eV; and Ar* $^3P_0$, 11.72 eV and $^3P_2$, 11.55 eV) were produced by impact of 70–120-eV electrons. For He* metastables, He*($2\,^1S$) atoms were quenched by a He discharge lamp (using the radiation of $\lambda=2.06$ μm) and the pure He*($2\,^3S$) spec-

trum was obtained. The He*($2\,^1S$) spectrum was derived by the difference between the two spectra with the quench lamp on and off. The Ne* and Ar* spectra are basically due to $^3P_2$ atoms [intensity ratio $I(^3P_2)/I(^3P_0)\sim 5$]. The ultraviolet photoemission spectra were measured with a conventional rare-gas–discharge source (He I, 21.22 eV; Ne I 16.67 eV; Ar I, 11.62 eV). A Grafoil sample was cleaned by heating under ultrahigh vacuum (10^{-8}–10^{-9} Torr) for 20 h. It consists of graphite crystallites with basal (cleavage) planes parallel to the foil surface.

III. RESULTS

Figure 2 shows the angle-resolved UPS of graphite measured with the geometry illustrated in the inset. The threshold with the maximum kinetic energy indicated by arrows corresponds to emission from the Fermi level E_F. In the He I spectrum, two peaks observed at 13.6 and 6.8 eV have been assigned to direct emissions from π and σ valence bands, respectively, of which the former consists of pure $2p_z$ (z; normal to the basal plane) atomic orbitals and the latter is based on sp^2-hybridized $2s$, $2p_x$, and $2p_y$ atomic orbitals.[4–7] Since the **k**-conservation rule comes into play in the direct emission, the peak positions referred to E_F move as the photon energy is changed (Fig. 2). With the decrease in the kinetic energy the background due to "true secondaries" rises up continuously. Two sharp bands at 2.9 and 3.8 eV are ascribed to final-state structures, reflecting the high density of σ^* conduction bands above E_F.[5–7] We cannot determine the crystal azimuth because of rotational disorder of our sample, but the spectral features observed here are consistent with previous photoemission data using a highly oriented pyrolytic graphite[4] or single crystals.[5–7]

Figure 3 shows the angle-resolved MAES of graphite measured with the same geometry as in the UPS. The thresholds with the maximum kinetic energy indicated by arrows are determined by the extrapolation of the curves and correspond to emission from the E_F. The MAES below ~ 5 eV exhibit very similar profiles as the UPS and therefore two stationary bands at 2.9 and 3.8 eV can be attributed to the σ^* conduction bands again. On the other hand, the MAES above ~ 5 eV show rather broad structures, which do not correspond to those in the UPS. Furthermore, the peak positions (A and B) referred to the threshold do not depend on the excitation energy of the metastable atoms. These observations indicate that the k-conservation rule is smeared out in contrast to the case of photoemission event, because the system involves the momentum of the incident metastable atom which is changed before and after ionization.

Before assigning the broad band structure, we should clarify the deexcitation channel. Here, one of the best ways to distinguish between the AD and RI+AN processes is to compare the He* ($2\,^1S$) and He* ($2\,^3S$) spectra: if the latter process is dominant, two spectra will give similar spectral features, whereas in the former case the difference in the excitation energy of the metastable atom will be reflected in the two spectra. Figure 3 clearly shows that He* metastable atoms decay on graphite via the AD process, because the threshold and peak positions shift by the difference in the excitation energy; 20.6 eV ($2\,^1S$) − 19.8 eV ($2\,^3S$) = 0.8 eV. In a previous paper,[2] it has been suggested that the He* ($2\,^3S$) atom deexcites on the graphite surface predominantly through the RI+AN process. However, this is not the case in the light of the

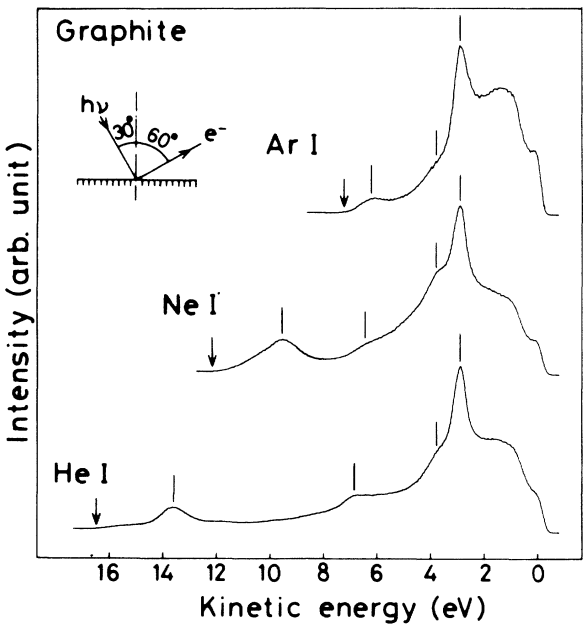

FIG. 2. Ultraviolet-photoemission spectra of graphite using He I, Ne I, and Ar I resonance lines.

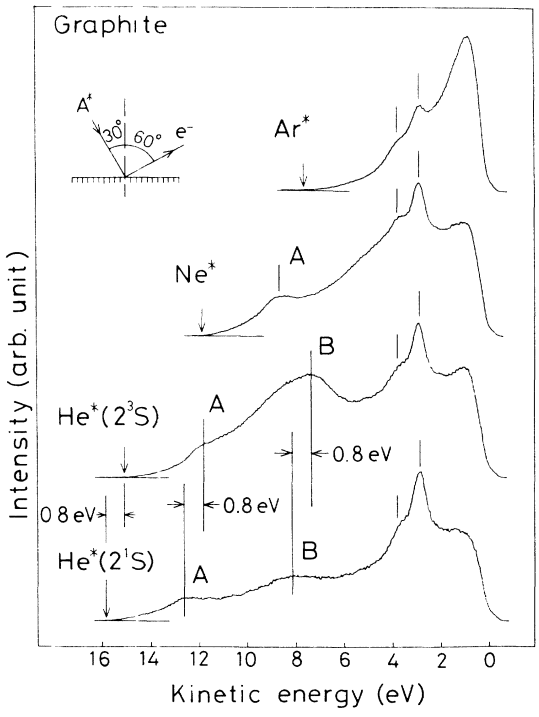

FIG. 3. Metastable-atom electron spectra of graphite using He* ($2\,^1S$), He* ($2\,^3S$), Ne*, and Ar* atoms.

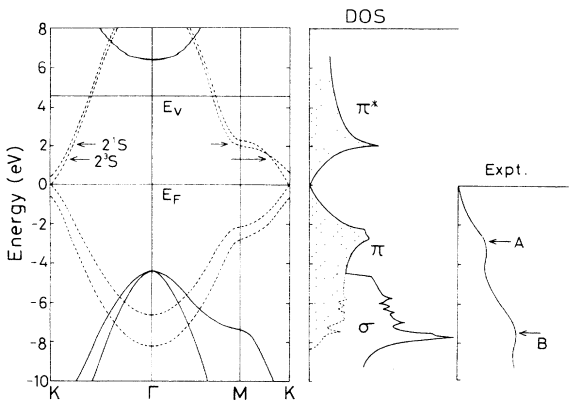

FIG. 4. Theoretical band structure, density of states (Ref. 8), and He* ($2\,^1S$) spectrum of graphite. The arrows in the band structure indicate the positions of the 2s levels for He* ($2\,^1S$) and He* ($2\,^3S$).

present, more complete study. The similar energy shifts relative to the He* MAES are observed in the Ne* and Ar* MAES, which indicates that the Ne* and Ar* atoms also deexcite via the AD process.

Figure 4 shows the theoretical band structure for three-dimensional graphite and the density of states (DOS) calculated by Kamimura *et al.* using discrete-variational (DV) $X\alpha$ linear confirmation of atomic orbitals (LCAO) approximation.[8] Similar band structures were calculated by Tatar *et al.*[9] and Holzwarth *et al.*,[10] and their basical features agree with one another. The solid and dotted curves represent σ and π bands, respectively. The He* ($2\,^1S$) MAES is also shown in the figure. From the comparison between the DOS and MAES, we find that (i) the observed maxima *A* and *B* correlate closely to the π DOS maxima derived from the flat parts near the symmetry point *M* and the bottoms at Γ, respectively, and (ii) the steep hump at -4.5 eV or the sharp peak at -7.7 eV based on the σ bands is almost missing in the MAES.

IV. DISCUSSION

First, we discuss the suppression of the RI process on the graphite surface. The transition rate for the RI process depends essentially on the spatial overlap between the 2s orbital of the metastable He* atom and the empty orbitals of the surface having the same energy as that of the 2s;

$$T_{\mathrm{RI}} \propto \sum_{\mathbf{k}'}^{\mathrm{unocc}} |\langle \phi_{2s}(\mathbf{r}) u_{\mathbf{k}'}(\mathbf{r}) \exp(i\mathbf{k}'\cdot\mathbf{r})\rangle|^2 , \tag{1}$$

where $u_{\mathbf{k}'}(\mathbf{r})$ is the amplitude of an unoccupied Bloch function with the wave vector $\mathbf{k}'$. The transition probability for the AD process, on the other hand, is given by[3]

$$T_{\mathrm{AD}} \propto \sum_{\mathbf{k}}^{\mathrm{occ}} |\langle u_{\mathbf{k}}(\mathbf{r}_1) \exp(i\mathbf{k}\cdot\mathbf{r}_1)\phi_{2s}(\mathbf{r}_2)|(1/r_{12})|\phi_{1s}(\mathbf{r}_1)\psi_E(\mathbf{r}_2)\rangle|^2 , \tag{2}$$

where $u_{\mathbf{k}}(\mathbf{r})$ is the amplitude of an occupied Bloch function and $\psi_E(\mathbf{r})$ is an orbital of the continuum state. On a metal or semiconductor surface having empty levels opposite the 2s orbital of the He* metastable atom [Fig. $1(a_1)$], the RI process depending on the overlap between the ϕ_{2s} and surface orbitals occurs before the AD process, which is essentially determined by the overlap between ϕ_{1s} and a surface orbital, because the ϕ_{2s} orbital (effective radius $r_{\mathrm{eff}} \sim 2.5$ Å) (Ref. 11) is much further extended to the surface than ϕ_{1s} ($r_{\mathrm{eff}} \sim 0.3$ Å).[12]

In this respect the present case seems to be puzzling at first sight, because graphite is semimetal with no band gap below the vacuum level and has empty levels at the energy position corresponding to that of the 2s level. This problem can be solved as follows. The ionization energy of the 2s electron of the He* atom near the surface is estimated by $E_i' - E_{\mathrm{ex}}'$, where E_i' and E_{ex}' are the effective ionization potential of the He atom and the effective excitation energy of the He* metastable atom near the surface, respectively. The value of E_i' is known to decrease by $\sim 1-2$ eV from its gas-phase value (24.6 eV) owing to the image potential,[1] while the values of E_{ex}' do not change much from their gas-phase values ($2\,^1S$, 20.6 eV; $2\,^3S$, 19.8 eV).[13] We thus obtain $E_i' - E_{\mathrm{ex}}' \sim (23.1-20.6)$ eV $= 2.5$ eV for the $2\,^1S$ atom and $(23.1-19.8)$ eV $= 3.3$ eV for the $2\,^3S$ atom, taking the effect of the image potential to be -1.5 eV. The energy positions of the 2s levels for the He* ($2\,^1S$) and He* ($2\,^3S$) are indicated by arrows in Fig. 4. As seen in the figure, the empty states of graphite corresponding to the 2s level of He* lie in the π^* bands near the symmetry points *M* ($k = 1.48$ Å^{-1}) and *K* ($k = 1.71$ Å^{-1}) in the Brillouin zone. The empty σ^* bands are located far above the energy region concerned. Figure 5 shows the real part of the π^* wave function at *M* for the graphite layer and the 2s atomic orbital of the He* metastable atom. At point *M*, all rows of the carbon atoms perpendicular to $\mathbf{k}$ have the same phase, but each double row shows a phase change. Since each carbon atom is thus surrounded by two atoms of the opposite phase and one atom of the same phase, the wave function at *M* cannot give an effective overlap integral (1) with widely extending 2s orbitals of the He* atoms. This is the reason for the suppression of the RI process in the state at point *M*. A similar argument can be made for the π^* wave function at point *K*.

In the case of Ne* and Ar* atoms the situation is rather complex, since the overlap integral (1) involves the anisotropic *p* orbitals of metastable atoms. The electron configurations of Ne* and Ar* are $(2p)^5(3p)^1$ and $(3p)^5(4p)^1$, respectively. The chemical-bond formation

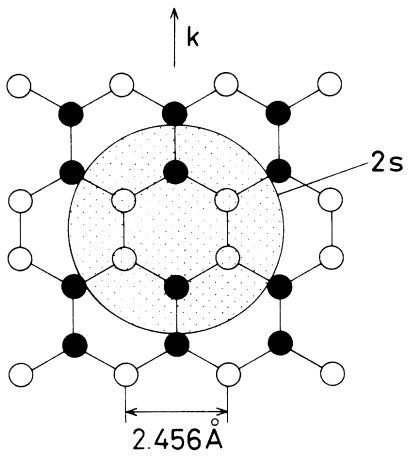

FIG. 5. Schematic view of the π^* wave function of the graphite layer at symmetry point M together with the $2s$ atomic orbital of the He* atom. The solid and open circles indicate positive and negative components of the C $2p_z$ wave function, respectively.

between the inner empty orbital of metastable atoms ($2p$ for Ne* and $3p$ for Ar*) and the occupied orbitals of the surface will cause the empty p lobe to orient to the surface. On the other hand, the outer unpaired orbital ($3p$ for Ne* and $4p$ for Ar*) favors the same direction as the inner empty orbital owing to the electron-electron repulsion. As a result, the Ne* (or Ar*) metastable atom approaches the surface with the unpaired p lobes directed to the surface. However, their lobes are much extended spatially and cannot give an effective overlap integral due to the phase mismatch as in the case for the $2s$ orbital mentioned above.

Next, we describe the electron distribution due to the valence bands. Since metastable atoms deexcite on graphite through the AD (or PI) process, the relative band intensity in the MAES largely depends on the overlap of the occupied Bloch function and the vacant $1s$ orbital of the He* atom. At sufficiently low collision energy ($\sim$40 meV for the present case), the effective region that should be taken into account in the above integral (2) is expected to be $\sim$3–5 Å outside the surface.[14] Therefore, a Bloch function such as the π (composed of C $2p_z$ atomic orbitals) protruding normal to the surface with large amplitude overlaps effectively with the $1s$ orbital of the He* atom and gives a strong band in the spectrum. On the other hand, the sp^2-hybridized σ functions distributed parallel to the surface layer and screened by the π functions give little contribution to the spectrum. The same propensity of the MAES has been found in thin layers of benzene[15] and pentacene[2] adsorbed parallel to the graphite surface. As is seen in Fig. 3, the relative intensity of band B in the He* ($2\,^3S$) MAES is much stronger than that in the He* ($2\,^1S$) MAES. This result may indicate that the $2\,^3S$ spectrum involves some contribution from the σ functions in addition to the π, because the $2\,^3S$ atoms can approach the surface more closely than the $2\,^1S$ atoms.[16] Finally, the intensity of the MAES features relative to the secondary-electron features below $\sim$5 eV in the He* ($2\,^1S$) spectrum are much weaker than that in the He* ($2\,^3S$) and Ne* spectra. This indicates that possibly some of He* ($2\,^1S$) atoms relax on the surface through the RI+AN process and give greater strength to the secondary features in the spectrum, since the $2s$ level of the He* ($2\,^1S$) atom locates near the π^* DOS maxima of graphite, while the highest occupied levels of He* ($2\,^3S$) and Ne* lie below the π^* DOS maxima (see Fig. 4).

The above results of graphite indicate that the selection of the deexcitation channel of the metastable atom (either RI+AN or AD) is governed not only by the energy position of empty levels at the solid surface relative to that of the highest occupied level of the metastable, but also by the spatial distribution of the empty orbitals at the surface. Further, electron emission via the AD process directly reflects the electron distribution of the occupied surface states. These features of metastable-atom electron spectroscopy provide a useful means of probing the spatial distribution of Bloch functions (both occupied and empty) localized on the solid surface.

ACKNOWLEDGMENTS

We thank Professor H. Kamimura, The University of Tokyo, for his helpful discussions.

[1]H. D. Hagstrum, in *Electron and Ion Spectroscopy of Solids*, edited by L. Fiermans, J. Vennik, and W. Dekeyser (Plenum, New York, 1978).
[2]Y. Harada, H. Ozaki, and K. Ohno, Phys. Rev. Lett. **52**, 2269 (1984).
[3]Y. Harada and H. Ozaki, Jpn. J. Appl. Phys. **26**, 1201 (1987).
[4]W. Eberhardt, I. T. McGovern, E. W. Plummer, and J. E. Fisher, Phys. Rev. Lett. **44**, 200 (1980).
[5]A. R. Law, J. J. Barry, and H. P. Hughes, Phys. Rev. B **28**, 5332 (1983).
[6]D. Marchand, C. Frétigny, M. Lagues, F. Batallan, Ch. Simon, I. Rosenman, and R. Pinchaux, Phys. Rev. B **30**, 4788 (1984).
[7]T. Takahashi, H. Tokailin, and T. Sagawa, Solid State Commun. **52**, 765 (1984); Phys. Rev. B **32**, 8317 (1985).
[8]C. Frétigny, R. Saito, and H. Kamimura (unpublished).
[9]R. C. Tatar and S. Rabii, Phys. Rev. B **25**, 4126 (1982).
[10]N. A. W. Holzwarth, S. G. Louie, and S. Rabii, Phys. Rev. B **26**, 5382 (1982).
[11]P. E. Siska, Chem. Phys. Lett. **63**, 25 (1979).
[12]S. Fraga, J. Karwowski, and K. M. S. Saxena, *Handbook of Atomic Data* (Elsevier, Amsterdam, 1976).
[13]Y. Harada, H. Ozaki, and K. Ohno, Solid State Commun. **49**, 71 (1984).
[14]B. Woratschek, W. Sesselman, J. Küppers, G. Ertl, and H. Haberland, Surf. Sci. **180**, 187 (1987).
[15]H. Kubota, T. Munakata, T. Hirooka, T. Kondow, K. Kuchitsu, K. Ohno, and Y. Harada, Chem. Phys. **87**, 399 (1984).
[16]S. W. Wang and G. Ertl, Surf. Sci. **93**, L75 (1980).